Investigation on the influence of geometric parameters of rectangular hollow cross-sections on buckling of the structure

Neha Arieckal Jacob, Dr. Sangarappillai Sivaloganathan

College of Engineering, UAE University, UAE

Abstract: *The effect of cross-sectional parameters on the local buckling behavior of a rectangular hollow section (RHS) under lateral compression is examined in this study through finite element modeling and optimization. The finite element model was first validated against experimental data. With good agreement observed between the experimental and FEA results, the validated FEA model in ABAQUS was used in conjunction with Isight to conduct an optimization study and examine the influence of cross-section parameters on the buckling behavior of the section. Cross-sectional parameters considered included the aspect ratio of the section, the thickness to width ratio of the web and the thickness to width ratio of the flange. For a target buckling load and given definite ranges of the width, height, flange thickness and web thickness, the best combination of parameters was arrived at using the optimization software Isight.*

Keywords: *local buckling, validation, parametric optimization, ABAQUS, Isight, RHS, lateral compression*

1. Introduction

This paper investigates the effects of the three parametric ratios (i) aspect ratio (ii) thickness to width ratio of the web and (iii) thickness to width ratio of the flange of a rectangular hollow section (RHS), on its buckling behavior when subjected to a compressive load in a direction perpendicular to the axis of the section. Motivation for this study can be described in the following way. Efficient structural members should have minimum material and weight while maintaining high strength and this is achieved by having maximized second moment of area of cross sections in beams. Thin walled hollow sections are an easy means to achieve this objective. Shell structures are widely encountered in many engineering applications and are commonly used in the aerospace, aeronautical and automobile industries. Although shell thinness demonstrates the high efficiency of shells that is associated with the shell's low weight and simultaneous high strength, a shell's thinness manifests itself in compression (Ventsel and Krauthammer, n.d.). Telescopic cantilevers are one such application of shell structures, which when subjected to a tip load, cause indirect compression due to shear in the overlap area between any two connected sections. These structural members can be treated as an assemblage of thin plates connected at their edges. These plates that make the assembly are susceptible to local buckling. This local buckling may be analyzed independently of the overall buckling of the structural member as adopted in this study. An RHS sample of aluminium with 140 mm length is used as the candidate for this study. The paper focuses on the use of the Finite Element Analysis software ABAQUS and the verification of the results with experimentation along with an optimization study using Isight.

There are two methods for investigating a stability problem (i) the Eigen value analysis and (ii) load deflection analysis. In the Eigen value method the critical load is obtained in essentially a single step. In the load deflection method the load is continuously increased while noting the deflection until the critical load is reached. The second method is laborious but permits the study of the entire history of load deflection. In this paper, only the first method is used. The rest of the paper describes a brief literature review and the formulation of the research method, the experimentation, Finite Element Analysis using ABAQUS, parametric analysis using Isight, analysis and discussion of the results and conclusions.

2. Literature Review and the Research Methodology

Plate structures are a special case of shell structures because shell theories are a generalization of plate theories(Laulusa et al., 2006). A shell is, in essence, a structure that can be derived from a plate, by initially forming the middle surface as a singly (or doubly) curved surface(Zienkiewicz and Taylor, n.d.). Shells in the form of rectangular hollow sections (RHS) can therefore be regarded as a combination of individual plate elements connected together to form the required shape.

In general, plates are classified according to the ratio w/t, where 'w' is the width of a plate in a plane and 't' is a plate thickness (Ventsel and Krauthammer, n.d.). Thin plates are the most extensive group, representing an intermediate type of plate, with 8 . . . 10 ≥ 'w/t' ≤ 80 . . . 100.

The strength of compression members like RHS, is thought to depend only on their slenderness ratio (w/t). Compression members in general can be classified into three groups: compact, non-compact, and slender. Yielding, inelastic buckling, and elastic buckling, respectively, control the ultimate strength of the members in each group(Yoo and Lee, n.d.). The current AASHTO (2007) has provisions for the limiting value of the width-to-thickness ratio (w/t) classifying the subpanels into these three groups. The validity of this requirement is, however, limited to bridge constructions and the accuracy has also been questioned in several investigations(Bedair, n.d.).

Investigation into the static analysis of thin-walled beams with open and closed sections has been carried out extensively through many studies(Saoula et al., 2016). However, at a certain level of the externally applied loads, the thin-walled members exhibit an instability leading to failure in the form of buckling. With the development of numerical tools as the finite element method, buckling of thin walled structures has been extensively studied and continues to be a topic of extensive research. Investigation on local buckling in particular has also gained considerable attention. Research includes the study of the local buckling behavior of many profiles including elliptical profiles in compression (McCann et al., 2016) (Silvestre, 2008), welded box section and I-section stub columns (Shi et al., 2016) and box sections (Liu et al., 2015).

Most compression tests aimed at studying either overall buckling (Theofanous et al., n.d.), (Theofanous and Gardner, 2009) or local buckling (H.X. et al., n.d.), (Shi et al., 2016), (Liu and Young, 2003) have been conducted for axial compression. In this investigation, compression of the RHS in a direction perpendicular to the axis of the beam will be studied.

Although it is widely accepted, in closed sections such as the hollow rectangular sections, for both flanges and webs, the local buckling depends on their respective width-thickness ratios (w/t), numerous parametric studies have been conducted to study the influence of other parameters on the buckling behavior of thin walled structures. Ban et al used a validated finite element model to perform a parametric study, considering different cross-sectional dimensions and column slenderness to better understand the overall buckling of the structure (Ban et al., 2013). The elasto-plastic local buckling behavior of the polygonal thin-walled steel sections was investigated analytically and experimentally to examine the effect of the width-thickness parameters, the aspect ratios, the bent angles, the number of sides of the polygonal structure on the buckling of the structure(Migita and Fukumoto, 1997). Even for composite thin-walled box members, the influence of length to height ratio, width to height ratio and ply angle have been studied for their influence on the behavior of structures (Ramkumar et al., 2010). Although many other studies have been conducted to better understand the influence of cross-sectional parameters on the behavior of structures (Kumar and Sahoo, 2016), (Ragheb, 2015), (Y.B. et al., n.d.), (Yuan et al., 2014), (Liu et al., 2015) and (Mohebkhah and Chegeni, 2012), no study to date appears to have conducted to study the influence of on the parameters of a rectangular hollow section that is loaded in compression transversally. This in turn has prompted this current study which has the following research question:

What are the effects of the three parametric ratios (i) aspect ratio (ii) thickness to width ratio of the web and (iii) thickness to width ratio of the flange of a rectangular hollow section (RHS), on its buckling behavior when subjected to a compressive load in a direction perpendicular to the axis of the section?

2.1 Research Methodology

The research methodology adopted has the following five steps:

1. Identify an instance of reality that will buckle in the elastic range and can be manufactured and experimentally tested to validate FEA results
2. Eigen value analysis
3. Conduct a compression test in the MTS machine to obtain the load-deflection (travel of the cross head) behaviour of the sample and carry out 5 replications to validate the ABAQUS model
4. Use Isight to carry out an optimization study to study the effects of the three parametric ratios using the validated ABAQUS model from step (3).
5. Analyse the results and draw conclusions.

2.2 Identification of the Instance of Reality

The instance of reality is the definition of the geometry of an RHS that will buckle before yielding and one that is manufacturable for testing with minimum cost. In order to arrive at such a cross section, an initial Eigen value analysis was carried out to obtain the buckling load value. With a load value just below the buckling load value obtained from the Eigen value analysis, a static stress analysis was performed on the same section and the maximum Von Mises value thus obtained was compared with the yield stress value of the material to be tested. A smaller Von Mises value confirmed elastic buckling. From the analysis, a section of 58.4mm x 28.4mm cross-section with a thickness of the flange (t_f) and web (t_w) of 1.2 mm was found to be the suitable Instance of Reality. The thickness of commercially available sections was then reduced in steps to match the thickness of the FEA models to ensure elastic buckling. The parent material for the test specimens was an RHS with external dimensions as 60mm x 30 mm and thickness of 2 mm. The length of the specimen was fixed at 140 mm so that it can lie within the plates of the MTS machine to apply a uniform pressure when loading. Figure 1 shows the instance of reality.

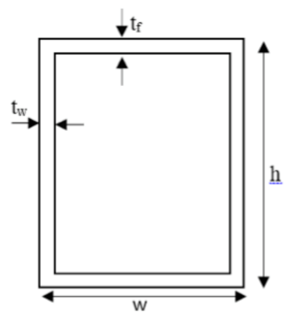

Figure 1. The Instance of reality.

3. Finite Element Modelling

The ABAQUS model was built to represent the instance of reality with the intention of validating the FEA model so that the model can be used further in an optimization study. The analysis presented here involves an elastic buckling analysis, details of which are shown subsequently.

3.1 Geometry and boundary conditions

The FE model comprised of three parts—the top and bottom end plates, and the aluminum RHS, with the two plates representing the upper and lower jaws of the MTS machine. The assembly of the FE model is as shown in Figure 2.

The bottom face of the RHS is assigned a frictional interaction with the bottom end plate which is encastred, thereby restricting all degrees of freedom of the bottom end plate. The top face of the RHS is also assigned a frictional interaction with the top end plate. A reference point, RP-1 was connected to the nodes on the top surface of the top plate via a kinematic coupling constraint available in ABAQUS. The top plate has all degrees of freedom restrained apart from vertical translation. A concentrated load was applied through this reference point, thus applying uniform pressure at the top edges of the top end plate.

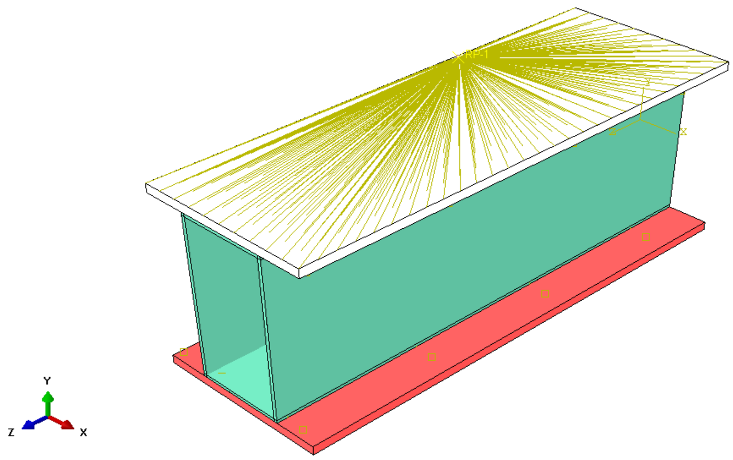

Figure 2. Assembly of FE model

3.2 Finite element mesh, element and material properties

In the FEM model, an eight-node linear brick elements with reduced integration (C3D8R) was used to model the steel end plates, while the aluminum RHS were modeled using the S4R, a 4-node reduced integration shell element. A mesh size of 5 mm × 5 mm was accurate enough to predict the behavior of the studied column and was used to mesh the RHS. The measured mechanical properties as listed in Table 2, were used for the rectangular hollow section. Poisson's ratio of aluminum alloy was assumed to be 0.3. For, the steel end plates, an elasticity modulus of 2.0×10^5 MPa and Poisson's ratio of 0.3 was used.

The analysis in ABAQUS was carried out in two steps. The first step was a static stress step where an initial point load of 1 kN was applied through RP-1. The second step was a linear perturbation step buckle using the Subspace solver.

3.3 Results

An Eigen value analysis was carried out for five models, with each model corresponding to one sample. The mode shapes and buckling load values for the first two modes of all five samples are shown in Table 1 and Figures 3-7 below.

Table 1. Analysis Buckling load values

	Buckling load: Mode 1 (kN)	Buckling load: Mode 2 (kN)
SAMPLE 1	20.77	21.99
SAMPLE 2	21.25	22.64
SAMPLE 3	20.77	21.99
SAMPLE 4	21.21	22.49
SAMPLE 5	21.51	22.88

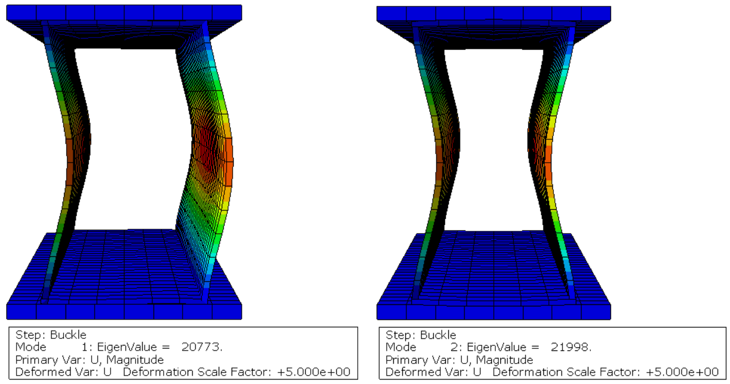

Figure 3. (L-R) Buckling Mode 1 and 2 for sample 1

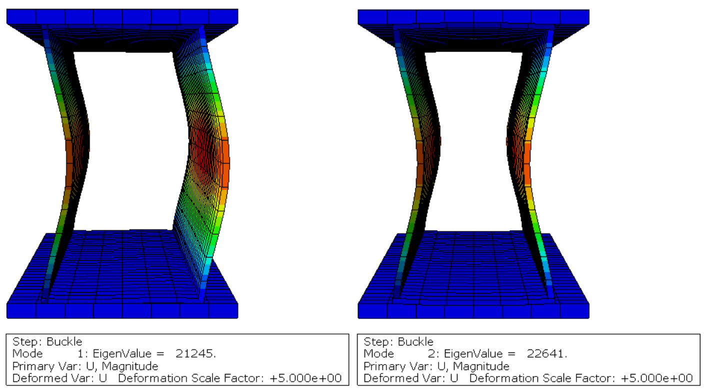

Figure 4. (L-R) Buckling Mode 1 and 2 for sample 2

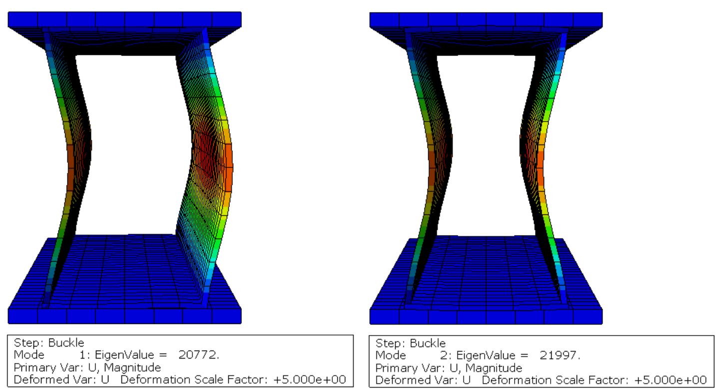

Figure 5. (L-R) Buckling Mode 1 and 2 for sample 3

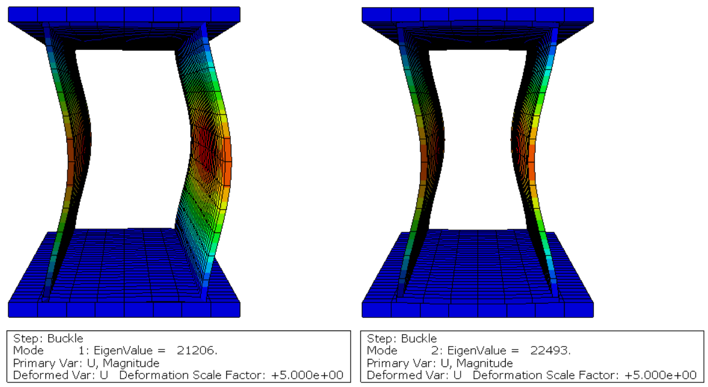

Figure 6. (L-R) Buckling Mode 1 and 2 for sample 4

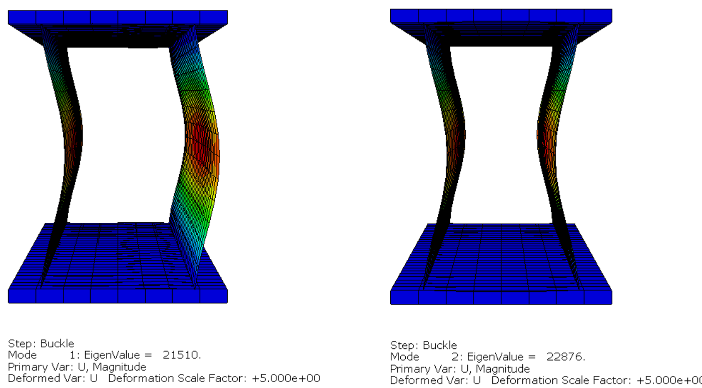

Figure 7. (L-R) Buckling Mode 1 and 2 for sample 5

4. Experimental Methods

An experimental study was conducted for the purpose of validation of the FEA ABAQUS model. In the following sections, test specimens and parameters, material properties, test setup and experimentation, and results of the experimental program are described.

4.1 Test specimens and parameters

A total of five rectangular hollow sections (RHS) were fabricated and tested under a compressive load. The bought out extruded RHS was cut to 140mm length with an initial outer cross-section of 60mm*30mm with a thickness of 2mm. In order to allow for buckling to take place within the elastic range, the thickness of the section was brought down to 1.2mm reducing the cross-section to 58.4mm*28.4mm. The reduction of thicknesses were done using a CNC machine.

For each specimen, the thicknesses at 10 different locations along each side of the cross-section was measured are shown in Figure 8. The averages of thickness ($t_{w(avg)}$ and $t_{f(avg)}$) and geometric dimensions are shown in Table 2, where the geometric symbols are defined according to Figure 1.

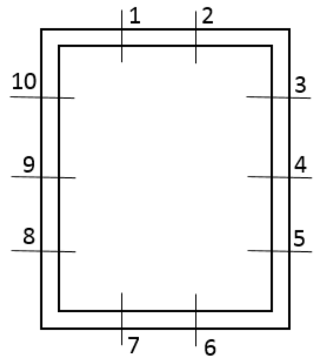

Figure 8. Thickness measurement location

Table 2. Average thickness of web and flange

	THICKNESS											
	t_1	t_2	t_6	t_7	$t_{f(avg)}$	t_3	t_4	t_5	t_8	t_9	t_{10}	$t_{W(avg)}$
SAMPLE 1	1.19	1.16	1.03	1.26		1.12	0.95	1.09	1.06	1.18	1.04	
	1.23	1.14	1.07	1.21	**1.14**	1.1	1.18	1.07	1.06	1.06	1.27	**1.10**
SAMPLE 2	1.18	1.13	1.0	1.15		1.08	1.0	1.15	1.16	1.21	1.04	
	1.13	1.24	1.0	1.14	**1.11**	1.07	1.16	1.16	1.18	1.15	1.06	**1.12**
SAMPLE 3	1.15	1.12	1.08	1.19		1.0	0.98	1.1	1.14	1.09	1.22	
	1.15	1.16	1.18	0.95	**1.14**	1.08	1.0	0.95	1.1	1.22	1.11	**1.10**
SAMPLE 4	1.27	1.14	0.95	0.98		1.13	1.17	1.08	1.21	1.04	1.11	
	1.29	1.16	1.01	0.99	**1.14**	1.13	1.19	1.05	1.21	1.07	1.11	**1.11**
SAMPLE 5	1.32	1.13	0.95	1.01		1.33	1.31	1.12	1.18	1.07	1.09	
	1.34	1.13	0.93	1.13	**1.13**	1.32	1.33	1.1	1.16	1.09	1.11	**1.12**

Although all the samples were to be reduced to a thickness of 1.20 mm, Table 2 is indicative of the variation of thickness along the section.

4.2 Material properties

To determine the material properties of the aluminum specimens, two tensile coupons as shown in Figure 9 were cut out from the length from which the samples for the compression tests were taken and tested in accordance with the Test Standards named in Table 3.

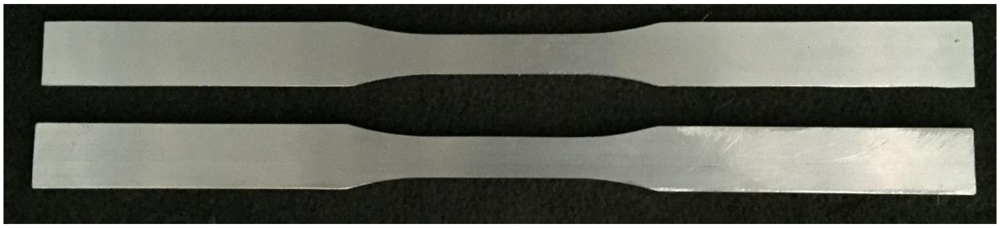

Figure 9. Test coupon for material properties

The average material properties are listed in Table 3, where 'E' is the Modulus of elasticity and 'd' is the density. These values were used as inputs to the ABAQUS model.

Table 3. Material properties test results

Standard	E (N/mm^2)	d (kg/m^3)
ASTM A 370-15	69087	-
ASTM D 792-00 Method A)	-	2643

4.3 Test set-up and experimentation

The compression tests were carried out at UAE University by means of an MTS testing machine (model: 20/MH). Each RHS was placed on the bottom plate of the machine and held in place by a compressive load applied by the top plate. A continuous load was applied until the RHS buckled, after which the load was released. On releasing the load, the specimen returned to its original shape, confirming elastic buckling. The instrumentation layout for the test is shown in Figure 10.

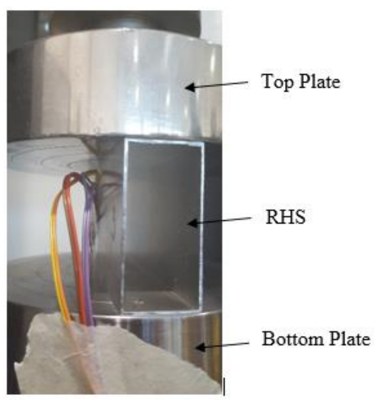

Figure 10. Test set-up

4.4 Results

The load vs displacement values were recorded and the graphs for all five samples are as shown in Figure 11. The buckled shapes of all the fives samples obtained experimentally are shown in Figure 12 below.

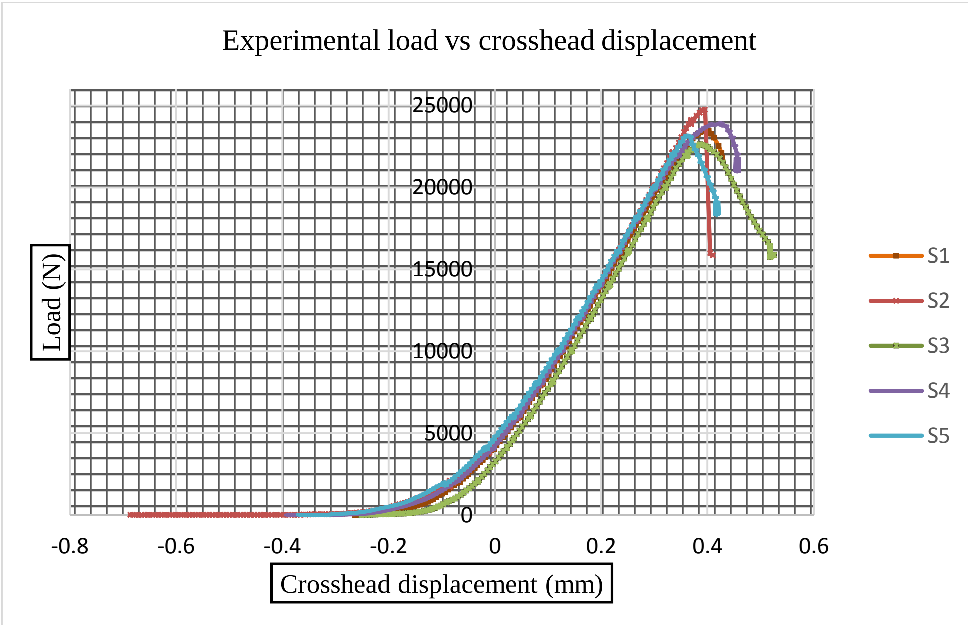

Figure 11. Load vs displacement graph of sample 1 to sample 5

Load against cross head displacement graphs shown in Figure 5 indicate that there is a zero error present in the load values applied by the machine. For all samples, zero displacement takes place around the 5 kN value, which means that contact between the upper plate of the MTS machine and the sample takes place at this load value. Therefore, the correct buckling load value should be the value given by the MTS machine (around 22 kN) minus the value at which contact takes place (around 5 kN). The corrected buckling values are given in Table 4. These values are used further in Table 5 for validation of the FEA model.

Table 4. Experimental buckling load values

	Buckling load(kN)	Zero Error (kN)	Corrected Buckling load (kN)
SAMPLE 1	23.49	4.26	19.23
SAMPLE 2	24.76	4.48	20.28
SAMPLE 3	22.63	3.28	19.35
SAMPLE 4	23.93	4.33	19.60
SAMPLE 5	23.18	4.82	18.36

The range of buckling load values varies from 18.36 kN to 20.28 kN as seen in Table 4. This can be attributed to the variation of thickness along the section as indicated in Table 2.

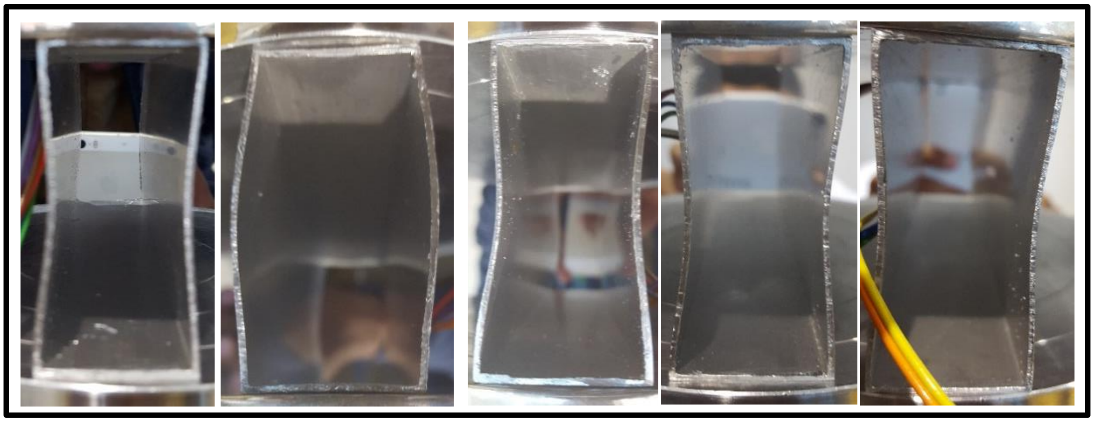

Figure 12. (L-R) Buckled shapes of samples 1 to 5

4.5 Analysis steps and validation of FEA model

The buckled shape of samples 1, 3, 4 and 5 matched with the shape of the second mode of the analysis. For sample 2, the mode shape was not a match. For all five samples, the buckling load values from the first mode of the analysis was slightly higher than that observed from the experiment. The maximum difference in the buckling load values was 23% with an average error of 14 % as tabulated in Table 5. The difference in the values between the analysis and the experiment can be attributed to variation in thickness across the cross-section and the fact that the average thickness value and not the minimum thickness value was taken for the analysis.

Table 5. Buckling load comparison

	BUCKLING LOAD (kN)		
	FEA (Mode1)	EXPERIMENTAL	Error%
SAMPLE 1	20.77	19.23	7.2%
SAMPLE 2	21.25	20.27	4.6%
SAMPLE 3	20.77	19.35	6.8%
SAMPLE 4	21.21	19.60	7.5%
SAMPLE 5	21.51	18.35	14.6%
	AVERAGE ERROR %		8.14%

The fact that the modes are similar in both the FEA and experimentation shows that the results predicated by FEA simulation is in agreement with the test results. This validated the FEA model and therefore it can be used in the parametric study ahead.

5. Parametric study

The validated ABAQUS model of the Aluminum RHS was used in Isight to study how various parameters or parametric ratios influenced the critical buckling load of the RHS. The model is created to manage optimization as shown in Figure 9.

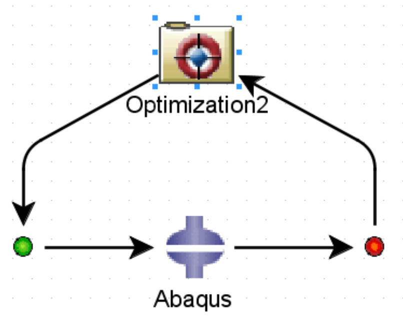

Figure 13. Isight Optimization Model

5.1 Problem definition

Over a certain range of allowable values for each of the parameters (Refer Figure 1) and given a target buckling load of 50 kN, with a minimum allowable value of 25 kN and maximum allowable value of 75 kN, the aim is to determine the best combination of values for a given set of conditions.

The permissible values for the input parameters are as follows:

1. Height 'h': 40, 41, 42, 43, 44 ……. 60
2. Width 'w': 20, 21, 22, 23, 24 ……. 40
3. Flange thickness 't_f': 1, 1.1, 1.2, 1.3, 1.4 ……… 2
4. Web thickness 't_w': 1, 1.1, 1.2, 1.3, 1.4 ……… 2

For these values of input parameters and given the target buckling load, the optimization study was run for five different conditions:

1. No condition on input parameters
2. $t_f = t_w$
3. $w/t_f > h/t_w$
4. $h/t_w > w/t_f$
5. $w/t_f = h/t_w$

5.2 Input and Output parameters

The (*.cae) file was used as input and the (*.odb) file was used as the output in the optimization model. As the model used in ABAQUS uses the perturbation step for buckling, Isight cannot read the buckling load values directly from ABAQUS. Therefore, a python script was written to calculate the buckling load corresponding to the first Eigen mode of the ABAQUS model. This script was read along with the (*odb) file. Once both these files are selected and read, the four geometric dimension properties are selected as input parameters. The buckling load is selected as the output parameter to be monitored. The ranges and targets for all these parameters are defined in the ABAQUS part of the loop.

5.3 Optimization Technique

The optimization model in Isight uses a Pointer technique which is an automatic optimization engine that controls a set of standard optimization techniques. It currently controls four optimization methods: a genetic algorithm, Nelder and Mead downhill simplex, sequential quadratic programming (NLPQL), and a linear solver. A hybrid combination of these methods solves a broad range of design optimization problems. The Pointer Automatic Optimizer can control one algorithm at a time or all four at once. As the optimization is proceeding, the technique determines which algorithms are most successful as well as optimal internal control parameters (step sizes, numbers of iterations, number of restarts, etc).

This technique is selected because it is well suited for long running simulations and non-linear design spaces.

5.4 Results

The results obtained for all five cases listed in section 5.1 are detailed in the Table 6 below.

Table 6. Optimum parametric values

Case No.	Condition	h (mm)	w (mm)	t_w (mm)	t_f (mm)	Buckling Load (kN)
1	NONE	40	30	1.1	1.4	50.059
2	$t_f = t_w$	44	22	1.2	1.2	49.416
3	$w/t_f > h/t_w$	46	40	1.5	1.0	50.158
4	$h/t_w > w/t_f$	40	22	1.2	1.0	49.869
5	$w/t_f = h/t_w$	40	40	1.2	1.2	51.683

6. Conclusions

It has been noted at the beginning that efficient structural members should have minimum material and weight while maintaining high strength. High strength is achieved by having maximized second moment of area (I) of cross sections in beams, and minimum material is achieved by having minimum cross-sectional area. Table 6 above, gives the optimum values for the given range of cross-sectional dimensions. For these values, the second moment of area and cross-sectional area are calculated and tabulated in Table 7 below.

Table 7. Geometric properties of cross-section

Case No.	Condition	I (mm^4)	A (mm^2)
1	NONE	37576.99	171.84
2	$t_f = t_w$	38584.88	152.64
3	$w/t_f > h/t_w$	72681.17	206
4	$h/t_w > w/t_f$	28737.71	128
5	$w/t_f = h/t_w$	46773.56	186.24

From a manufacturing point of view, a section with the minimum cross-sectional area will result in maximum savings. Also, lower the cross-sectional area, lower the weight of the section and therefore lower the dead weight of the machine. Increasing the dead weight of the machine can lead to many disadvantages. Keeping this in mind, a section with the minimum area is preferred. In this case, minimum area is achieved in case no. 4, which in this case also results in minimum second moment of area (I). The second case where the flange thickness and web thickness are the same and equal to 1.2 mm is a good compromise as this is easy to manufacture as well. However, the final decision is case dependent.

7. References

1. Ban, H., Shi, G., Shi, Y., Bradford, M.A., 2013. Experimental investigation of the overall buckling behaviour of 960 MPa high strength steel columns. J. Constr. Steel Res. 88, 256–266. doi:10.1016/j.jcsr.2013.05.015
2. Bedair, O., n.d. Design expression for web shear buckling of box sections by accounting for flange restraints. Journal of Constructional Steel Research 110, 163–169. doi:10.1016/j.jcsr.2015.02.018
3. H.X., Y., Y.Q, W., T, C., X.X, D., Y.D, B., Y.J, S., n.d. Local buckling and post-buckling strength of extruded aluminium alloy stub columns with slender I-sections. Thin-Walled Structures.
4. Kumar, N., Sahoo, D.R., 2016. Optimization of lip length and aspect ratio of thin channel sections under minor axes bending. Thin-Walled Struct. 100, 158–169. doi:10.1016/j.tws.2015.12.015
5. Laulusa, A., Bauchau, O.A., Choi, J.-Y., Tan, V.B.C., Li, L., 2006. Evaluation of some shear deformable shell elements. Int. J. Solids Struct. 43, 5033–5054. doi:10.1016/j.ijsolstr.2005.08.006
6. Liu, M., Zhang, L., Wang, P., Chang, Y., 2015. Buckling behaviors of section aluminum alloy columns under axial compression. Eng. Struct. 95, 127–137. doi:10.1016/j.engstruct.2015.03.064
7. Liu, Y., Young, B., 2003. Buckling of stainless steel square hollow section compression members. J. Constr. Steel Res. 59, 165–177. doi:10.1016/S0143-974X(02)00031-7
8. McCann, F., Fang, C., Gardner, L., Silvestre, N., 2016. Local buckling and ultimate strength of slender elliptical hollow sections in compression. Eng. Struct. 111, 104–118. doi:10.1016/j.engstruct.2015.12.020
9. Migita, Y., Fukumoto, Y., 1997. Local buckling behaviour of polygonal sections. J. Constr. Steel Res., South and South East Asia Regional Issue 41, 221–233. doi:10.1016/S0143-974X(97)00008-4
10. Mohebkhah, A., Chegeni, B., 2012. Local–global interactive buckling of built-up I-beam sections. Thin-Walled Struct. 56, 33–37. doi:10.1016/j.tws.2012.03.018
11. Ragheb, W.F., 2015. Local buckling of welded steel I-beams considering flange–web interaction. Thin-Walled Struct. 97, 241–249. doi:10.1016/j.tws.2015.09.026
12. Ramkumar, K., Ganesan, N., Kannan, R., 2010. Global and local behaviour based composite damping studies on thin-walled box structure. Eur. J. Mech. - ASolids 29, 253–265. doi:10.1016/j.euromechsol.2009.09.003

13. Saoula, A., Meftah, S.A., Mohri, F., Daya, E.M., 2016. Lateral buckling of box beam elements under combined axial and bending loads. J. Constr. Steel Res. 116, 141–155. doi:10.1016/j.jcsr.2015.09.009
14. Shi, G., Xu, K., Ban, H., Lin, C., 2016. Local buckling behavior of welded stub columns with normal and high strength steels. J. Constr. Steel Res. 119, 144–153. doi:10.1016/j.jcsr.2015.12.020
15. Silvestre, N., 2008. Buckling behaviour of elliptical cylindrical shells and tubes under compression. Int. J. Solids Struct. 45, 4427–4447. doi:10.1016/j.ijsolstr.2008.03.019
16. Theofanous, M., Chan, T.M., Gardner, L., n.d. Structural response of stainless steel oval hollow section compression members. Engineering Structures.
17. Theofanous, M., Gardner, L., 2009. Testing and numerical modelling of lean duplex stainless steel hollow section columns. Eng. Struct. 31, 3047–3058. doi:10.1016/j.engstruct.2009.08.004
18. Ventsel, E., Krauthammer, T., n.d. Introduction to the General Shell Theory, in: Thin Plates and Shells. p. 307.
19. Ventsel, E., Krauthammer, T., n.d. Thin Plates and Shells: Theory, Analysis and Applications.
20. Y.B., S., Y, K., R. Budarapu, P., n.d. Parametric studies on buckling of thin walled channel beams. Computational Material Science 96, Part B, 416–424. doi:10.1016/j.commatsci.2014.07.058
21. Yoo, C.H., Lee, S.C., n.d. Energy Methods, in: Stability of Structures: Principles and Applications. p. 412.
22. Yuan, H.X., Wang, Y.Q., Gardner, L., Shi, Y.J., 2014. Local–overall interactive buckling of welded stainless steel box section compression members. Eng. Struct. 67, 62–76. doi:10.1016/j.engstruct.2014.02.012
23. Zienkiewicz, O.., Taylor, R.L., n.d. Shells as an assembly of flat elements, in: The Finite Element Method: Solid Mechanics.